

## Pattern Generation by Dissipative Parametric Instability

A. M. Perego,<sup>1,2,\*</sup> N. Tarasov,<sup>1,3</sup> D. V. Churkin,<sup>1,4,5</sup> S. K. Turitsyn,<sup>1,4</sup> and K. Staliunas<sup>2,6</sup>

<sup>1</sup>*Aston Institute of Photonic Technologies, Aston University, Birmingham B4 7ET, United Kingdom*

<sup>2</sup>*Departament de Física i Enginyeria Nuclear, Universitat Politècnica de Catalunya, E-08222 Barcelona, Spain*

<sup>3</sup>*Institute of Computational Technologies SB RAS, Novosibirsk 630090, Russia*

<sup>4</sup>*Novosibirsk State University, Novosibirsk 630090, Russia*

<sup>5</sup>*Institute of Automation and Electrometry SB RAS, Novosibirsk 630090, Russia*

<sup>6</sup>*Institució Catalana de Recerca i Estudis Avançats, Passeig Lluís Companys 23, E-08010 Barcelona, Spain*

(Received 14 September 2015; published 13 January 2016)

Nonlinear instabilities are responsible for spontaneous pattern formation in a vast number of natural and engineered systems, ranging from biology to galaxy buildup. We propose a new instability mechanism leading to pattern formation in spatially extended nonlinear systems, which is based on a periodic antiphase modulation of spectrally dependent losses arranged in a zigzag way: an effective filtering is imposed at symmetrically located wave numbers  $k$  and  $-k$  in alternating order. The properties of the dissipative parametric instability differ from the features of both key classical concepts of modulation instabilities, i.e., the Benjamin-Feir instability and the Faraday instability. We demonstrate how the dissipative parametric instability can lead to the formation of stable patterns in one- and two-dimensional systems. The proposed instability mechanism is generic and can naturally occur or can be implemented in various physical systems.

DOI: 10.1103/PhysRevLett.116.028701

The formation of patterns in nonlinear physical and biological systems represents the conceptually important idea of how simple objects can self-evolve into complex structures through instabilities. Spontaneous pattern formation in a variety of nonlinear spatially extended systems is initiated by modulation instabilities (MIs): the homogeneous state becomes unstable with respect to growing spatial modulation modes in a given range of wave numbers [1]. Possibly the best-known class of MI is the Benjamin-Feir (BF) instability, originally introduced in fluid dynamics [2,3] and later identified in different areas of science, such as plasmas [4], nonlinear optics [5–7], and other fields (see, for example, the review [1]). The physical essence of the BF instability is that some spatial modulation modes with symmetric wave numbers  $k$  and  $-k$  can synchronize with the strong homogeneous mode with  $k = 0$  due to a nonlinear frequency shift in self-focusing (modulationally unstable) media, and, thus, can experience exponential growth.

Another fundamental MI—ubiquitous in physics—is the Faraday instability, which has been known since even before the BF instability. This instability results from the periodic modulation in time of an appropriate dispersive parameter of the system [8]. Faraday unstable modes oscillate at half the frequency of the parametric forcing. The Faraday instability can be understood as a synchronization of the growing modes at  $k$  and  $-k$  with the homogeneous mode through the periodic parametric driving. Specifically, when a parameter is time modulated at frequency  $2\omega_0$ , the modes grow if their wave numbers  $k$  and  $-k$  satisfy the nonlinear dispersion relation  $\omega_0 = \omega(k)$ .

The Faraday instability has been observed in a variety of systems: it was originally seen in vertically shaken fluids [8], and later in periodically modulated chemical systems [9], vertically shaken granular media [10], periodically modulated Bose condensates [11,12], and nonlinear fiber optics. In the latter case, the modulation of nonlinearity or dispersion in time (piecewise or in a continuous manner) can initiate instability [13–16] and lead to pattern formation [17–19]. Typically, the Faraday instabilities and patterns are studied in BF-stable systems. However, they can also appear as additional instabilities in BF-unstable cases [20].

In this Letter, we propose a new type of instability, which we call the dissipative parametric instability. While it shares some features with the BF and Faraday instabilities, the dissipative parametric instability is also very distinct from these two classical cases.

In various applications, both the BF and Faraday instabilities and the associated nonlinear pattern formation can be described using a very generic model, the complex Ginzburg-Landau equation [21] (CGLE), which (in the case of one spatial dimension) reads

$$\frac{\partial A}{\partial t} = \mu A + (b - id) \frac{\partial^2 A}{\partial x^2} + (ic - s)A|A|^2, \quad (1)$$

where  $A(t, x)$  is the complex field amplitude distributed in space  $x$  and evolving in time  $t$ ,  $\mu$  is the gain coefficient,  $s$  and  $c$  are the saturation and nonlinearity coefficients, and  $b$  and  $d$  are the diffusion and diffraction coefficients. In the case of Faraday instability, diffraction  $d(t)$  and/or nonlinearity  $c(t)$  are periodic functions of time. Note that the

modulation in time of dissipative parameters, such as  $\mu$ ,  $s$ , or the diffusion  $b$  (which effectively acts as dissipation for large  $k$  components), does not result in Faraday instability. In conservative systems, such as nonlinear fibers and Bose-Einstein condensates, both the BF and Faraday instabilities are studied within the framework of the nonlinear Schrödinger equation (NLSE), the conservative limits of the CGLE.

The linear stability of the homogeneous solution of the CGLE with periodic coefficients can be studied using the Floquet stability analysis. The homogeneous state  $A_{\text{hs}} = A_0 \exp(ic|A_0|^2 t)$ , in which  $\mu = s|A_0|^2$ , is weakly perturbed by modulation modes  $a_{+k}(t) \exp(ikx)$  and  $a_{-k}(t) \exp(-ikx)$ , such that  $a_{+k}(t)$ ,  $a_{-k}(t) \ll |A_0|^2$ . Calculating numerically the amplitudes of perturbations after one modulation period, building a matrix map of a resonator round-trip, and diagonalizing it (see Supplemental Material [22] for details) allows us to calculate the Floquet multipliers  $F$ . A mode  $k$  is considered unstable when at least one of the absolute values of its multipliers is greater than 1. In order to visualize the instability spectrum, we plotted  $\max(|F(k)|)$ .

The BF instability, in the CGLE and in its conservative limit (NLSE), is a long-wave instability, because the band of unstable wave numbers always extends from  $k = 0$ ; see Fig. 1(a). For particular systems, e.g., those described by the Manakov equations [23] or the Lugiato-Lefever equation [24], BF is not purely a long-wave instability; i.e., its spectrum can slightly detach from  $k = 0$ . The Faraday instability is a short-wave instability: the area of unstable modes is clearly detached from the axis  $k = 0$ ; see Fig. 1(c). There are multiple Faraday instability tongues. In the first tongue, the growing modes oscillate with half the frequency of the parametric drive; in the second tongue, they oscillate with the frequency of the drive, and so on. Another fundamental difference is that BF-unstable modes grow monotonically, as shown in Fig. 1(b), whereas the growth of Faraday unstable modes is oscillatory and synchronized with the parametric drive, as in Fig. 1(d) (see also the Supplemental Material [22]).

The new type of instability—dissipative parametric instability—occurs in systems in which dissipative terms are periodically modulated in time in an antiphase (zigzag) manner with respect to  $k$  and  $-k$  modes; see Fig. 2(a).

First, the complex field evolves nonlinearly and homogeneously in time according to the CGLE with nonmodulated coefficients. Next, spectral losses are imposed over the wave number range  $-\Delta k$  at time instant  $t = T_f/2$ . Then a new stage of homogeneous nonlinear evolution takes place, followed by spectral losses over the wave number range  $+\Delta k$  at  $t = T_f$ . Note that the unmodulated dissipation in the  $k$  domain [constant diffusion coefficient  $b$  in Eq. (1)] or the symmetrically (for  $k$  and  $-k$  modes) modulated dissipation does not result in any instability. Additionally, we would like to point out that the dissipative

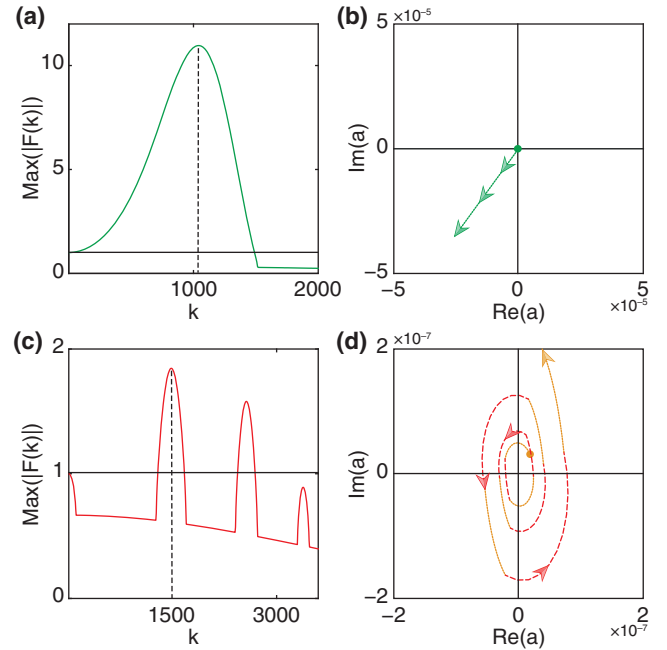


FIG. 1. (a),(c) Floquet spectrum calculated using the Floquet stability analysis of the homogeneous solution of the CGLE; instability occurs above the horizontal continuous line. (b),(d) The dynamics of complex amplitude  $a(k)$  of the most unstable mode (indicated by dashed vertical lines on the instability spectrum) is calculated by direct integration of the CGLE. Arrows indicate the direction of temporal evolution. The parameters used are  $\mu = 1$ ,  $s = 0.3$ ,  $b = 0.1 \times 10^{-6}$ , with full integration time  $T = 1$ . In the case of the BF instability [(a),(b)]  $c = 1$ ,  $d = -3 \times 10^{-6}$ . In the case of the Faraday instability [(c),(d)]  $c = 4.85$ ,  $d_1 = 5 \times 10^{-6}$ ,  $d_2 = 1 \times 10^{-6}$ ; a piecewise modulated diffraction coefficient is also considered, i.e.,  $d = d_1$  for  $0 < t < 0.2$  [orange line on (d)],  $d = d_2$  for  $0.2 < t < 0.4$  (red line), and so on.

term remains positive on average at every instant of time; i.e., the losses are never converted into gain.

Such antiphase spectrally modulated losses can occur in periodic (cyclic) systems with spectrally shifted dissipative components. In the one-dimensional case, dissipative parametric instability can arise in transmission fiber systems, lasers, or amplifiers, in which dissipative elements (such as filters) are imposed in alternating (zigzag) order in the frequency domain [25,26]. A laser is a natural example of a system exhibiting dissipative parametric instability if the frequency reflectivity profile of one mirror is shifted with respect to that of the other mirror; see Fig. 2(b). Such detuning results in periodic antiphase losses at every half-cavity round-trip.

Another possibility is to implement alternating losses in the wave number domain. This could be realized in transverse nonlinear optics, such as self-imaging resonators [27] or self-imaging arrays of lenses, if access is possible to the far field distribution at different positions along the resonator. Selective losses for the  $+k$  and  $-k$  components

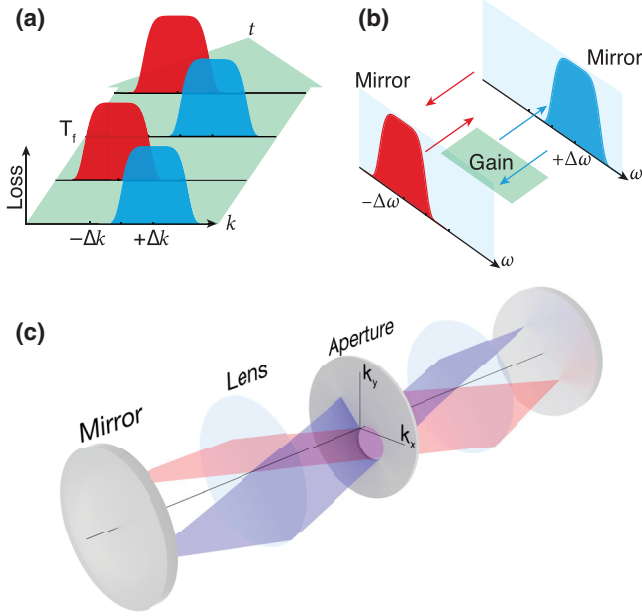


FIG. 2. (a) Dissipative parametric instability arises if periodic-in-time losses are introduced asymmetrically in the  $k$  domain, so that the modes with only positive or negative wave vectors are damped every half of the period  $T_f$ . (b) Dissipative parametric instability can be realized by alternating losses in the frequency domain, i.e., in a laser with detuned (in frequency) cavity mirrors. (c) A self-imaging resonator or self-imaging array of lenses with spatial filter displaced relative to the system's axis is another possibility.

can be imposed by placing corresponding spatial filters; see Fig. 2(c). The dissipative parametric instability could also be implemented in dissipative Bose-Einstein atomic or exciton-polariton condensates in semiconductor microcavities [28]. In the first case, velocity- (momentum-) resolved losses have to be imposed; in the second case, Bragg mirrors with suitable reflectivity profiles must be used [Fig. 4(a), Supplemental Figs. 5(a) and 5(c)[22]].

We calculated the properties of the dissipative parametric instability in a system described by Eq. (1), modeling without loss of generality the dissipative elements as super-Gaussian spectral filters,  $f_{1,2}(k) = \exp[-(k \pm k_0)^8/\sigma^8]$ . The specific spectral shape of the filter function is not critical for the properties of the dissipative parametric instability. We performed the Floquet analysis for losses that were periodic in time and antiphase in the  $k$  domain (see Fig. 3). The parameters used in the calculations are  $\mu = 1$ ,  $s = 0.2$ ,  $c = 3.5$ ,  $b = 0.1 \times 10^{-6}$ ,  $d = 5 \times 10^{-6}$ ,  $k_0 = 1822.1$ , and  $\sigma = 1885$ ; the modulation period is fixed,  $T_f = 2$ , except in Fig. 3(d) where  $T_f$  has been varied.

The dissipative parametric instability band starts from  $k = 0$ , Fig. 3(a), which makes its spectrum similar to the BF instability [compare with Fig. 1(a)]. We stress that the system considered on average as well as in every instant of time remains in the BF-stable regime. At the same time, the dissipative parametric instability spectrum has several

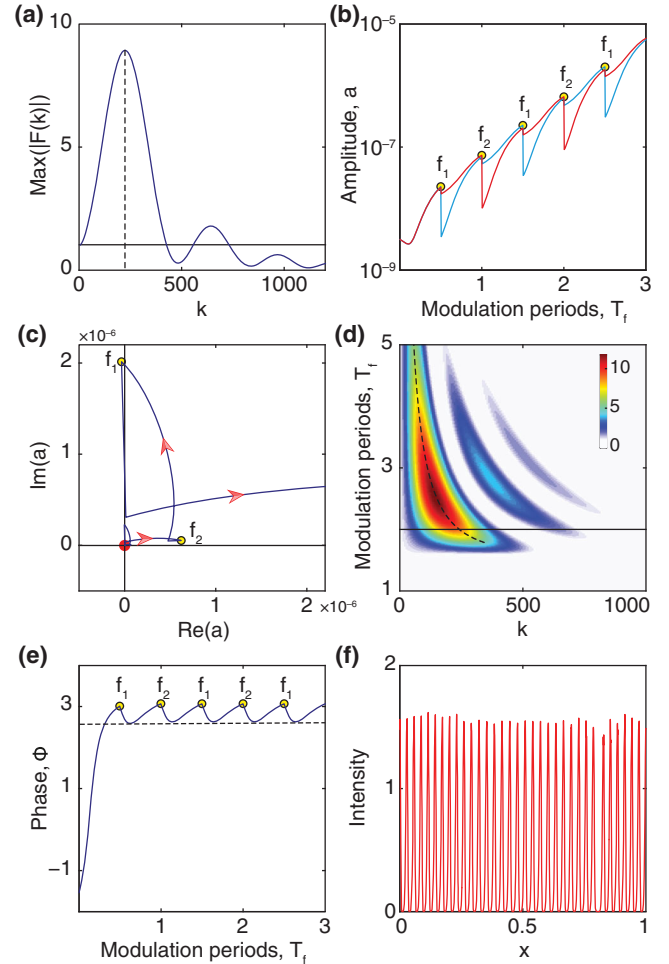


FIG. 3. (a) Spectrum of the dissipative parametric instability. The dashed line indicates the most unstable mode. (b) Evolution of the absolute values of the amplitudes of the most unstable modes  $a(k)$  and  $a(-k)$  (red and blue lines, respectively). The losses are introduced at points  $f_1, f_2$ , etc., in time. (c) The complex amplitude of the mode  $a(k)$  evolves in loops in phase space synchronized with external forcing. (d) Spectrum of the dissipative parametric instability as a function of the modulation period  $T_f$ ; the dashed line is the analytically estimated scaling law of the instability. (e) The generalized phase  $\Phi$  locks to the optimum value (dashed line), the point at which the mode's amplitudes are growing at the fastest rate, through periodic reset of the phase at instances of time at which the losses are applied. (f) Asymptotically stable pattern in a one-dimensional system.

tongues, as in Fig. 3(a) and 3(d), which is characteristic to the Faraday instability. We note that the dissipative parametric instability spectrum could be also tailored to make modes with small wave numbers stable, or to modify the number of instability tongues by changing the dissipation function, such as its shift over frequency and the modulation period over time.

As in Fig. 3(b), on average, the amplitudes of the unstable modes grow exponentially, but they oscillate synchronously with the external forcing like in the case

of the Faraday instability and unlike the monotonic evolution of BF instability (see Supplemental Fig. 1[22] for comparison). The complex amplitudes of the modulation modes perform looping in the phase space synchronized with the external modulation of dissipation, as in Fig. 3(c). The evolution in the phase space for the dissipative parametric instability is different from the cases of both the BF and Faraday instabilities.

Despite the fact that, similar to the BF case, modes with wave numbers close to zero are unstable [see Figs. 3(a) and 3(d)], the dissipative parametric instability exhibits different scaling laws compared to the BF instability. Indeed, whereas in the case of BF instability the instability spectrum does not scale over the modulation period (system length) [7], the scaling is well pronounced in the case of dissipative parametric instability, as depicted in Fig. 3(d). To characterize the scaling law, we phenomenologically assumed the parametric resonance condition, as for the Faraday instability, by imposing that the first unstable mode oscillates in time at frequency  $\omega_f/2$ , with  $\omega_f$  as the frequency of the forcing and where wave number  $k_{\text{inst}}$  is related to  $\omega_f/2$  through the dispersion relation. The resulting analytically derived scaling law (see the Supplemental Material [22]) coincides well with the numerical calculation, Fig. 3(d).

How and why the dissipative parametric instability emerges becomes clear through the calculation of the generalized phase  $\Phi = \varphi_{+k} + \varphi_{-k} - 2\varphi_0$ , where  $\varphi_{+k}$  and  $\varphi_{-k}$  are the phases of the modes with wave numbers  $+k$  and  $-k$ , respectively, and  $\varphi_0$  is the phase of the homogeneous mode. For a BF-stable system, if the dissipation is not modulated, the generalized phase  $\Phi$  evolves freely over time; this results in periodical growth and decay of amplitudes of modulation modes depending on the instantaneous phase, in such a way that the period-average amplitude remains the same. In the conservative limit, such periodically oscillating modes are well known under the name of Bogoliubov–De Gennes excitations (i.e., the sound waves of a condensate) [29].

The situation is completely different when the modes at  $+k$  or  $-k$  are periodically damped in a zigzag fashion. In this case, at the instant of time during which the damping is applied the generalized phase is reset to the value at which the amplitude is growing; see Fig. 3(e). Despite the increased dissipation on average, the exponential growth of the unstable modes sets in. We directly checked that such dynamics cannot be sustained if both modes were damped in phase. In this way, the dissipative parametric instability is fundamentally different from the Faraday instability, where the modes at  $+k$  and  $-k$  are modulated in phase.

The dissipative parametric instability eventually leads to pattern formation. For one-dimensional systems, we provide an example, in Fig. 3(f), of a stable pattern evolved from the homogeneous solution. The character of the final patterns crucially depends on nonlinearity through the

saturation of the amplitudes of unstable modes. Typically, stable and regular periodic patterns are excited; however, depending on the parameters, dynamic irregular patterns are observed, which are characterized by a permanent creation and annihilation of the pulselike localized structures during the temporal evolution (see Supplemental Fig. 4 [22]).

The increase in nonlinearity leads to a decrease of the wave number of the modulation pattern; the increase of the modulation period  $T_f$  and the dispersion coefficient  $d$  have the same effect, in agreement with Supplemental Eq. (9) [22].

Furthermore, an increase of the filters' width or a reduction of their separation leads to a lower modulation wave number; however, a minimum separation is needed in order to excite the instability.

More comments on the patterns' characterization, stability, and temporal evolution can be found in the Supplemental Material [22].

The dissipative parametric instability is of generic nature and could also be realized in higher-dimensional systems. An example is a two-dimensional system that is stable with respect to the BF instability, and where we apply the profile of the dissipation function in a zigzagging manner, as depicted in Fig. 4(a). As a result [see Fig. 4(b)], the dissipative parametric instability appears with a corresponding instability spectrum and leads to pattern

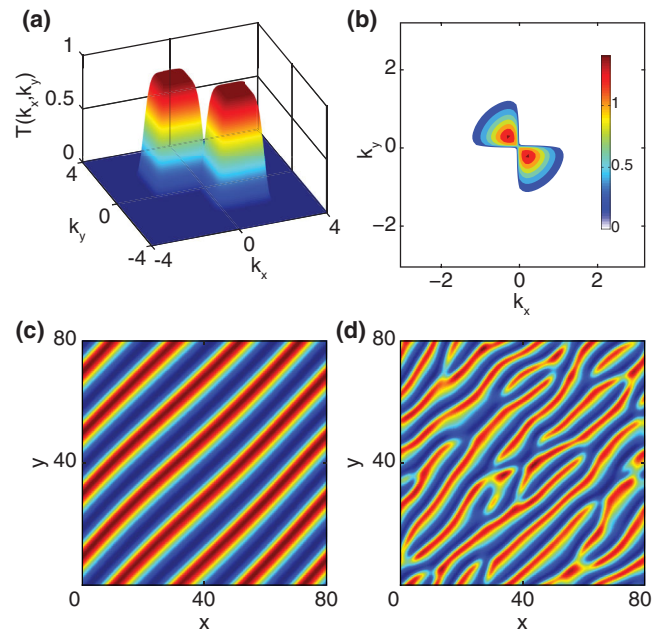


FIG. 4. (a) Zigzagging losses in wave number space  $(k_x, k_y)$ , (b) the instability area in  $(k_x, k_y)$  space as obtained by the Floquet analysis, and (c) 2D intensity patterns. Parameters are  $\mu = 0.2$ ,  $d = 0.05$ ,  $b = 0.08$ ,  $c = 0.35$ ,  $s = 0.3$ ,  $T_f = 5\pi$ , and  $\sigma = 1.0905$ . Losses are centered at  $k_{0x} = -1$ ,  $k_{0y} = +1$ . (d) By setting  $b = 0$ , the pattern becomes irregular in space and nonstationary in time.

formation. Different patterns could be obtained depending on the system parameters, varying from completely stable and regular modulation patterns, as in Fig. 4(c), to irregular ones, as in Fig. 4(d). The resulting periodic patterns in saturated regimes (when they are stable) are of wave numbers within the area in  $k$  space, where the losses are modulated. The dissipative parametric instability in 2D spatial systems could be controlled by managing the shape of the dissipation function with significant flexibility. (Further examples of two-dimensional patterns are reported in the Supplemental Material [22]).

In conclusion, we proposed and examined the dissipative parametric instability, a novel type of instability that can lead to pattern formation. The dissipative parametric instability occurs as a result of the periodic-in-time anti-phase (zigzagging) modulation of the spectral losses in the wave number (or frequency) domain. We have shown that this novel instability can lead to the formation of stable patterns in one- and two-dimensional systems. The dissipative parametric instability is generic and can occur in various physical systems, including fiber optics, lasers, and Bose-Einstein condensates.

We acknowledge support from the Spanish Ministerio de Educación y Ciencia, the European FEDER Project No. FIS2011-29731-C02-01, the ERC project ULTRALASER, the Russian Ministry of Education and Science (Grant No. 14.B25.31.0003), the Russian Foundation for Basic Research (Grant No. 15-02-07925), a Presidential Grant for Young Researchers (Grant No. 14.120.14.228-MK), and the Dinasty Foundation. N. T. is supported by the Russian Science Foundation (Grant No. 14-21-00110). A. M. P. acknowledges support from the ICONE Project through the Marie Curie Grant No. 608099.

---

\*Corresponding author.  
peregoa@aston.ac.uk

- [1] M. C. Cross and P. C. Hohenberg, *Rev. Mod. Phys.* **65**, 851 (1993).
- [2] T. B. Benjamin and J. E. Feir, *J. Fluid Mech.* **27**, 417 (1967).
- [3] D. J. Benney and A. C. Newell, *J. Math. Phys. (N.Y.)* **46**, 133 (1967).
- [4] J. F. Drake, P. K. Kaw, Y. C. Lee, G. Schmid, C. S. Liu, and M. N. Rosenbluth, *Phys. Fluids* **17**, 778 (1974).
- [5] V. I. Bespalov and V. I. Talanov, *Pis'ma Zh. Eksp. Teor. Fiz.* **3**, 471 (1966) [*JETP Lett.* **3**, 307 (1966)].

- [6] V. E. Zakharov and L. A. Ostrovsky, *Physica (Amsterdam)* **238D**, 540 (2009).
- [7] G. P. Agrawal, *Nonlinear Fiber Optics* (Academic Press, San Diego, 2006).
- [8] M. Faraday, *Phil. Trans. R. Soc. London* **121**, 299 (1831).
- [9] V. Petrov, Q. Ouyang, and H. L. Swinney, *Nature (London)* **388**, 655 (1997).
- [10] F. Melo, P. B. Umbanhowar, and H. L. Swinney, *Phys. Rev. Lett.* **72**, 172 (1994).
- [11] K. Staliunas, S. Longhi, and G. J. de Valcárcel, *Phys. Rev. Lett.* **89**, 210406 (2002); K. Staliunas, S. Longhi, and G. J. de Valcárcel, *Phys. Rev. A* **70**, 011601 (2004).
- [12] P. Engels, C. Atherton, and M. A. Hoefer, *Phys. Rev. Lett.* **98**, 095301 (2007).
- [13] M. Matera, A. Mecozzi, M. Romagnoli, and M. Settembre, *Opt. Lett.* **18**, 1499 (1993).
- [14] J. C. Bronski and J. N. Kutz, *Opt. Lett.* **21**, 937 (1996).
- [15] N. Smith and N. J. Doran, *Opt. Lett.* **21**, 570 (1996).
- [16] M. Droques, A. Kudlinski, G. Bowmans, G. Martinelli, and A. Mussot, *Opt. Lett.* **37**, 4832 (2012).
- [17] F. Kh. Abdullaev, S. A. Darmanyan, S. Bischoff, and M. P. Sørensen, *J. Opt. Soc. Am. B* **14**, 27 (1997).
- [18] K. Staliunas, C. Hang, and V. V. Konotop, *Phys. Rev. A* **88**, 023846 (2013).
- [19] M. Conforti, A. Mussot, A. Kudlinski, and S. Trillo, *Opt. Lett.* **39**, 4200 (2014).
- [20] M. Centurion, M. A. Porter, Y. Pu, P. G. Kevrekidis, D. J. Frantzeskakis, and D. Psaltis, *Phys. Rev. Lett.* **97**, 234101 (2006).
- [21] I. S. Aranson and L. Kramer, *Rev. Mod. Phys.* **74**, 99 (2002).
- [22] See Supplemental Material at <http://link.aps.org/supplemental/10.1103/PhysRevLett.116.028701> for more details on the stability analysis methods, analytical estimation of the instability frequency, and one- and two-dimensional pattern formation.
- [23] F. Baronio, M. Conforti, A. Degasperis, S. Lombardo, M. Onorato, and S. Wabnitz, *Phys. Rev. Lett.* **113**, 034101 (2014).
- [24] M. Haelterman, S. Trillo, and S. Wabnitz, *Opt. Lett.* **17**, 745 (1992).
- [25] S. Pitois, C. Finot, L. Provost, and D. J. Richardson, *J. Opt. Soc. Am. B* **25**, 1537 (2008).
- [26] K. Sun, M. Rochette, and L. R. Chen, *Opt. Express* **17**, 10419 (2009).
- [27] K. Staliunas and V. J. Sánchez-Morcillo, *Transverse patterns in nonlinear optical resonators* (Springer, Berlin, 2003).
- [28] I. Carusotto and C. Ciuti, *Rev. Mod. Phys.* **85**, 299 (2013).
- [29] L. Pitaevskii and S. Stringari, *Bose-Einstein Condensation* (Clarendon Press, Oxford, 2004).